

Reverse Shocks in Short Gamma-Ray Bursts

– The case of GRB 160821B and prospects as gravitational-wave counterparts –

Gavin P Lamb¹

¹ School of Physics and Astronomy, University of Leicester, University Road, Leicester, LE1 7RH, UK
E-mail: gpl6@leicester.ac.uk

ABSTRACT

The shock system that produces the afterglow to GRBs consists of a forward- and a reverse-shock. For short GRBs, observational evidence for a reverse-shock has been sparse – however, the afterglow to GRB 160821B requires a reverse-shock at early times to explain the radio observations. GRB 160821B is additionally accompanied by the best sampled macronova without a gravitational-wave detection, and an interesting late time X-ray afterglow behaviour indicative of a refreshed-shock. The presence of an observed reverse-shock in an on-axis short GRB means that the reverse-shock should be considered as a potential counterpart to gravitational-wave detected mergers. As a gravitational-wave counterpart, the afterglow to an off-axis GRB jet can reveal the jet structure – a reverse-shock will exist in these structured jet systems and the signature of these reverse-shocks, if observed, can indicate the degree of magnetisation in the outflow. Here we show the case of GRB 160821B, and how a reverse-shock will appear for an off-axis observer to a structured jet.

KEY WORDS: Yamada conference LXXI: proceedings — gamma-ray bursts: GRB 160821B, general — gravitational wave: electromagnetic counterparts

1. Introduction

For a relativistic shell expanding into a medium, two shocks will form; a forward shock that propagates into the external medium, and a reverse shock that propagates into the shell [Sari & Piran(1995)]. In describing the reverse shock, two regimes are usually discussed, these are the thin shell, or Newtonian shock case, and the thick shell, or relativistic shock case [Kobayashi(2000), etc]. The relativistic shell will decelerate at the reverse shock crossing time in both regimes [Kobayashi et al.(1999)]. The duration and energetics of short gamma-ray bursts (GRBs) imply that any reverse shock in these systems will typically be described by the thin shell case [Lamb & Kobayashi(2018), 2019].

Emission from a reverse shock is an important probe of the conditions in a GRB outflow towards the central engine. Modelling the observed afterglow emission enables constraints to be placed on the magnetisation and the bulk Lorentz factor Γ_0 , where $F_{max,r} = \Gamma_0 F_{max,f} C_F R_B$, and here F_{max} is the maximum synchrotron flux from the reverse and forward shock, r and f respectively, C_F is a correction factor, see [Harrison & Kobayashi(2013)], and $R_B \equiv \varepsilon_{B,r}/\varepsilon_{B,f}$ is the magnetisation parameter, see [Zhang et al.(2003)].

The reverse shock in short GRBs has been notori-

ously difficult to observe [Lloyd-Ronning(2018)], however, the short GRB 051221A has evidence¹ of a reverse shock with a radio frequency detection and upper-limits [Soderberg et al.(2006)], and recently reverse shock emission has been shown to be consistent with the optical afterglow to the candidate short GRB 180418A [Becerra et al.(2019)], and radio observations of the afterglow to the short GRB 160821B require a reverse shock component [Lamb et al.(2019a), Troja et al.(2019a)]. These successes in observing the reverse shock in short GRBs, although rare, raise the prospect of identifying the reverse shock emission in gravitational-wave detected neutron star mergers, where the systems jet-axis is likely misaligned for an observer and so the afterglow and GRB will be observed off-axis [Lamb & Kobayashi(2017), 2018, 2019].

2. GRB 160821B

The short GRB 160821B, at a redshift of $z = 0.162$, had an isotropic gamma-ray energy of $E_{\gamma,iso} = (2.1 \pm 0.2) \times 10^{50}$ erg, based on the 8–10,000 keV band fluence of $(2.52 \pm 0.19) \times 10^{-6}$ erg cm⁻² [Lü et al.(2017)]. X-

^{*1} GPL thanks Alexander van der Horst for kindly pointing out this paper in a comment following the conference talk

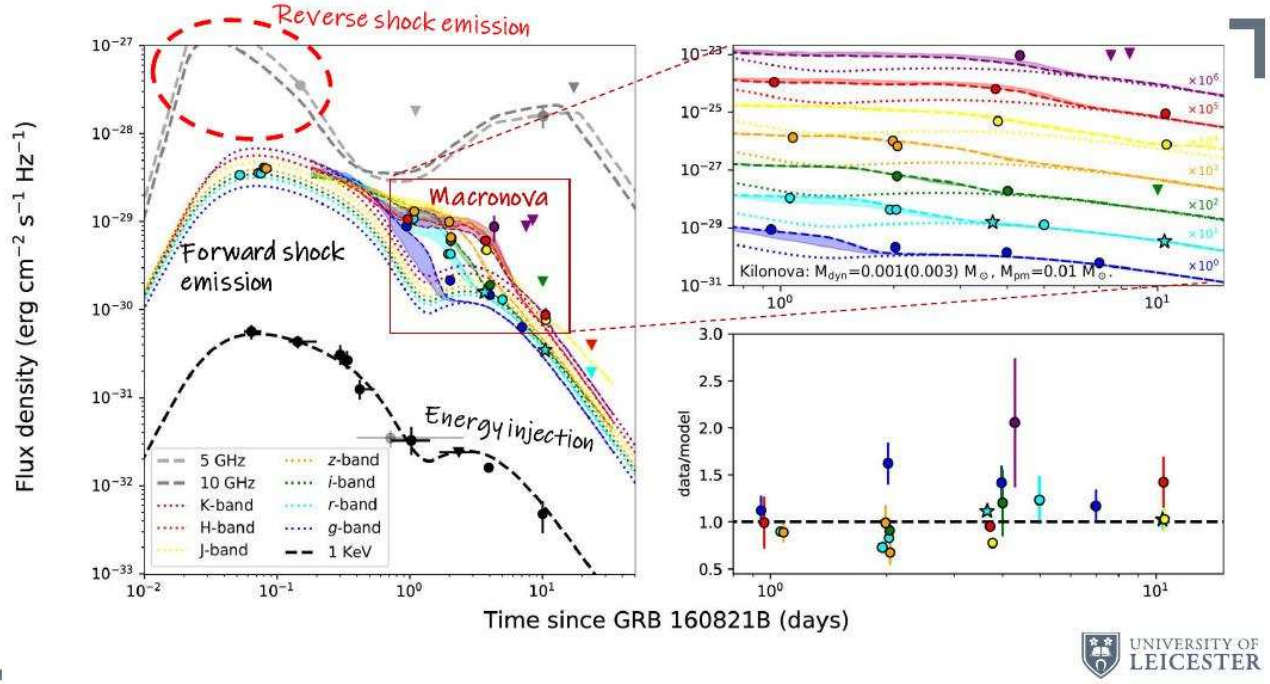


Fig. 1. The broadband afterglow to GRB 160821B. Dashed or dotted lines are the model light-curves, filled circles are data, and triangles upper-limits, see [Lamb et al.(2019a)] for details. Left: the afterglow from radio to X-ray frequencies (top to bottom), a reverse shock contribution is required at early times to explain the radio observation, while at late times energy injection is needed to explain the X-ray, optical and radio data. From ~ 1 –5 days an excess at optical and infrared indicates a macronova. Right top: expands the macronova and afterglow model with the data. Right bottom: shows the model fits versus data residual.

ray, optical, and radio frequency observations of the afterglow to GRB 160821B were performed from 0.06–23.23 days after the burst; for a full list of the observations used here see [Lamb et al.(2019a)]. Early infrared observations put limits on the presence of a macronova [Kasliwal et al.(2017)], however, more complete broadband observations revealed emission at optical and infrared frequencies in excess of that expected from afterglow modelling of the X-ray and radio data [Lamb et al.(2019a), Troja et al.(2019a)].

In Fig. 1 we show the afterglow data and our preferred model. The complex behaviour of the afterglow is explained variously by: the contribution of a reverse shock travelling into a mildly magnetised ($R_B \sim 8$) shell at early times (~ 0.1 days), we estimate a bulk Lorentz factor for the initial outflow $\Gamma_0 \sim 60$; a jet break at ~ 0.3 – 0.4 days followed by an injection of energy from a fallback powered second jet episode [Rosswog(2007), Kagawa et al.(2019)]² that rebrightens the afterglow [Granot et al.(2003), etc]; and a macronova contribution at ~ 1 –5 days. The best-fitting macronova model [Kawaguchi et al.(2018)] con-

sists of two-components: a dynamical ejecta mass of $\sim 0.001 M_\odot$, and a post-merger or secular ejecta mass of $\sim 0.01 M_\odot$.

3. Reverse Shocks as Gravitational Wave Counterparts

The GRB 170817A and its macronova and afterglow in association with the gravitational-wave detected merger of a binary neutron star at ~ 40 Mpc [Abbott et al.(2017)] has shown that short GRBs are produced in binary neutron star mergers. The late-time afterglow to GRB 170817A indicated that the resultant jets from neutron star mergers, when viewed at a higher inclination than the central jet axis, will reveal the outflow structure [Lamb & Kobayashi(2017)]. The post-peak rapid decline of the late-time afterglow [Lamb et al.(2019b), Troja et al.(2019b)], along with VLBI observations [Ghirlanda et al.(2019), Mooley et al.(2018)], cleared any ambiguity in the jet-core dominated origin of the afterglow [Lamb et al.(2018)].

For neutron star mergers discovered via gravitational-waves, the reverse shock in the afterglow can potentially be observed for systems that are inclined $< 20^\circ$, at a luminosity distance < 100 Mpc, and that have some lateral structure; see Fig 2 and [Lamb & Kobayashi(2019)].

^{*2} This second jet episode is slower than the initial GRB creating jet and likely responsible for the X-ray extended emission lasting ~ 300 s following the main burst

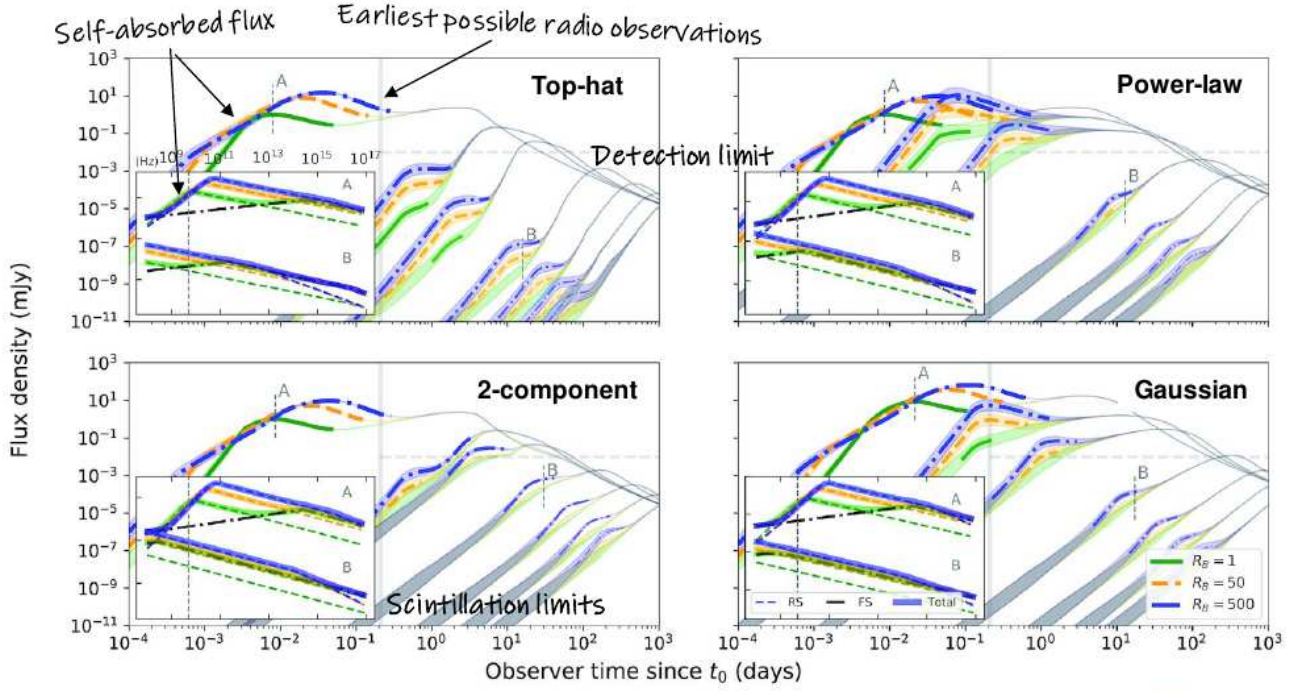


Fig. 2. The afterglow light-curve for four jet structure models following those in [Lamb & Kobayashi(2017)] but including sideways expansion, synchrotron self-absorption, and a reverse shock for an ejecta shell characterised by a magnetic parameter $R_B = [1, 50, 500]$, bold lines in green (solid), yellow (dashed), and blue (dash-dotted) respectively, see [Lamb & Kobayashi(2019)]. The light-curves for an afterglow at 5 GHz and 100 Mpc are shown at $[0^\circ, 12^\circ, 18^\circ, 36^\circ, 54^\circ, 72^\circ, 90^\circ]$. The effects of scintillation are shown with the grey shaded regions at early times while the size emitting region is still small [Granot & van der Horst(2014)]. Insets on each panel show the spectra at the times indicated by 'A' and 'B'.

Additionally, a magnetisation parameter $R_B \sim$ a few is required and observations should ideally commence at ~ 0.1 days post merger and at radio frequencies < 100 GHz. For such cases, scintillation may complicate the observations, however, carefully measured scintillation can be used to constrain the size of the emitting region [Granot & van der Horst(2014)].

References

- [Abbott et al.(2017)] Abbott, B. P., Abbott, R., Abbott, T. D., et al. 2017, ApJL, 848, L12
- [Becerra et al.(2019)] Becerra, R. L., Dichiaro, S., Watson, A. M., et al. 2019, ApJ, 881, 12
- [Ghirlanda et al.(2019)] Ghirlanda, G., Salafia, O. S., Paragi, Z., et al. 2019, Science, 363, 968
- [Granot et al.(2003)] Granot, J., Nakar, E., & Piran, T. 2003, Nature, 426, 138
- [Granot & van der Horst(2014)] Granot, J., & van der Horst, A. J. 2014, PASA, 31, e008
- [Harrison & Kobayashi(2013)] Harrison, R., & Kobayashi, S. 2013, ApJ, 772, 101
- [Kagawa et al.(2019)] Kagawa, Y., Yonetoku, D., Sawano, T., et al. 2019, ApJ, 877, 147
- [Kasliwal et al.(2017)] Kasliwal, M. M., Korobkin, O., Lau, R. M., et al. 2017, ApJL, 843, L34
- [Kawaguchi et al.(2018)] Kawaguchi, K., Shibata, M., & Tanaka, M. 2018, ApJL, 865, L21
- [Kobayashi et al.(1999)] Kobayashi, S., Piran, T., & Sari, R. 1999, ApJ, 513, 669
- [Kobayashi(2000)] Kobayashi, S. 2000, ApJ, 545, 807
- [Lamb & Kobayashi(2017)] Lamb, G. P., & Kobayashi, S. 2017, MNRAS, 472, 4953
- [Lamb & Kobayashi(2018)] Lamb, G. P., & Kobayashi, S. 2018, MNRAS, 478, 733
- [Lamb et al.(2018)] Lamb, G. P., Mandel, I., & Resmi, L. 2018, MNRAS, 481, 2581
- [Lamb & Kobayashi(2019)] Lamb, G. P., & Kobayashi, S. 2019, MNRAS, 489, 1820
- [Lamb et al.(2019a)] Lamb, G. P., Tanvir, N. R., Levan, A. J., et al. 2019a, ApJ, 883, 48
- [Lamb et al.(2019b)] Lamb, G. P., Lyman, J. D., Levan, A. J., et al. 2019b, ApJL, 870, L15
- [Lloyd-Ronning(2018)] Lloyd-Ronning, N. 2018, Galaxies, 6, 103
- [Lü et al.(2017)] Lü, H.-J., Zhang, H.-M., Zhong, S.-Q., et al. 2017, ApJ, 835, 181

- [Mooley et al.(2018)] Mooley, K. P., Deller, A. T.,
Gottlieb, O., et al. 2018, *Nature*, 561, 355
- [Rosswog(2007)] Rosswog, S. 2007, *MNRAS*, 376, L48
- [Sari & Piran(1995)] Sari, R., & Piran, T. 1995, *ApJL*,
455, L143
- [Soderberg et al.(2006)] Soderberg, A. M., Berger, E.,
Kasliwal, M., et al. 2006, *ApJ*, 650, 261
- [Troja et al.(2019a)] Troja, E., Castro-Tirado, A. J.,
Becerra González, J., et al. 2019a, *MNRAS*, 489, 2104
- [Troja et al.(2019b)] Troja, E., van Eerten, H., Ryan, G.,
et al. 2019b, *MNRAS*, 489, 1919
- [Zhang et al.(2003)] Zhang, B., Kobayashi, S., &
Mészáros, P. 2003, *ApJ*, 595, 950